Microlens array fabricated using electrohydrodynamic instability and surface properties

You-Jin Lee,[1] Young Wook Kim,[1] Young-Ki Kim,[1] Chang-Jae Yu,[1,2] Jin Seog Gwag,[3] and Jae-Hoon Kim[1,2,*]

[1]*Department of Information Display Engineering, Hanyang University, Seoul 133-791, South Korea*
[2]*Department of Electronic Engineering, Hanyang University, Seoul 133-791, South Korea*
[3]*Department of Physics, Yeungnam University, Geongsangbuk-Do 712-746, South Korea*
[*]jhoon@hanyang.ac.kr

Abstract: We fabricated polarization-dependent and polarization-independent microlens arrays (MLA) through the electrohydrodynamic instability of the optically anisotropic organic layer. The anisotropic flow induced by the instability of the organic layer leads to making the lens profile on the patterned electrode. We can easily control the polarization dependence of the MLA by controlling the surface alignment properties, even with the optically anisotropic organic layer. This method is a straightforward, fast, and reliable process for MLA fabrication since it does not require cumbersome developing and molding processes.

©2011 Optical Society of America

OCIS codes: (230.0230) Optical devices; (220.0220) Optical design and fabrication.

References and links

1. J. Arai, H. Kawai, and F. Okano, "Microlens arrays for integral imaging system," Appl. Opt. **45**(36), 9066–9078 (2006).
2. Y. Tanaka, M. Yamagata, Y. Komma, S. Mizuno, and K. Nagashima, "Lens design for optical head compatible with compact disk and digital versatile disk," Jpn. J. Appl. Phys. **37**(Part 1, No. 4B), 2179–2183 (1998).
3. K. Rastani, C. Lin, and J. S. Patel, "Active-fiber star coupler that uses arrays of microlenses and liquid-crystal modulators," Appl. Opt. **31**(16), 3046–3050 (1992).
4. M. T. Gale, J. Pedersen, H. Schütz, H. Povel, A. Gandorfer, P. Steiner, and P. N. Bernasconi, "Active alignment of replicated microlens arrays on a charge-coupled device imager," Opt. Eng. **36**(5), 1510–1517 (1997).
5. T. Okamoto, M. Mori, T. Karasawa, S. Hayakawa, I. Seo, and H. Sato, "Ultraviolet-cured polymer microlens arrays," Appl. Opt. **38**(14), 2991–2996 (1999).
6. D. Daly, R. F. Stevens, M. C. Hutley, and N. Davies, "The manufacture of microlenses by melting photoresist," Meas. Sci. Technol. **1**(8), 759–766 (1990).
7. J. Chen, W. Wang, J. Fang, and K. Varahramyan, "Variable-focusing microlens with microfluidic chip," J. Micromech. Microeng. **14**(5), 675–680 (2004).
8. N. S. Ong, Y. H. Koh, and Y. Q. Fu, "Microlens array produced using hot embossing process," Microelectron. Eng. **60**(3-4), 365–379 (2002).
9. S.-M. Kim and S. Kang, "Replication qualities and optical properties of UV-moulded microlens arrays," J. Phys. D Appl. Phys. **36**(20), 2451–2456 (2003).
10. X.-C. Yuan, W. X. Yu, N. Q. Ngo, and W. C. Cheong, "Cost-effective fabrication of microlenses on hybrid sol-gel glass with a high-energy beam-sensitive gray-scale mask," Opt. Express **10**(7), 303–308 (2002), http://www.opticsinfobase.org/oe/abstract.cfm?URI=oe-10-7-303.
11. C. S. Lim, M. H. Hong, Y. Lin, Q. Xie, B. S. Luk'yanchuk, A. S. Kumar, and M. Rahman, "Microlens array fabrication by laser interference lithography for super-resolution surface nanopatterning," Appl. Phys. Lett. **89**(19), 191125 (2006).
12. H. R. Stapert, S. del Valle, E. J. K. Verstegen, B. M. I. van der Zande, J. Lub, and S. Stallinga, "Photoreplicated anisotropic liquid-crystalline lenses for aberration control and dual-layer readout of optical discs," Adv. Funct. Mater. **13**(9), 732–738 (2003).
13. T. Scharf, "Static birefringent microlenses," Opt. Lasers Eng. **43**(3-5), 317–327 (2005).
14. M. He, X. Yuan, N. Q. Ngo, W. C. Cheong, and J. Bu, "Reflow technique for the fabrication of an elliptical microlens array in sol-gel material," Appl. Opt. **42**(36), 7174–7178 (2003).
15. D. B. Do, N. D. Lai, C. Y. Wu, J. H. Lin, and C. C. Hsu, "Fabrication of ellipticity-controlled microlens arrays by controlling the parameters of the multiple-exposure two-beam interference technique," Appl. Opt. **50**(4), 579–585 (2011).

16. E. Schaffer, T. Thurn-Albrecht, T. P. Russell, and U. Steiner, "Electrically induced structure formation and pattern transfer," Nature **403**(6772), 874–877 (2000).
17. E. Schäffer, T. Thurn-Albrecht, T. P. Russell, and U. Steiner, "Electrohydrodynamic instabilities in polymer films," Europhys. Lett. **53**(4), 518–524 (2001).
18. M. D. Dickey, E. Collister, A. Raines, P. Tsiartas, T. Holcombe, S. V. Sreenivasan, R. T. Bonnecaze, and C. G. Willson, "Photocurable pillar arrays formed via electrohydrodynamic instabilities," Chem. Mater. **18**(8), 2043–2049 (2006).

1. Introduction

The microlens array (MLA) is a key component for various optical systems, such as integral imaging for 3D displays, optical data storage, optical communication, and charge-coupled devices [1–4]. MLAs are categorized into two types - optically isotropic or anisotropic MLA (OIMLA or OAMLA) - depending on polarization dependence. Most MLAs show optically isotropic characteristics because they are made of optically isotropic materials, such as UV curable polymer, photoresist, or polydimethylsiloxane [5–7]. OIMLAs are fabricated by reflow, hot embossing, UV molding, photo-lithography using a gray scale mask, and laser interference lithography [6,8–11]. OAMLAs have been studied due to their axially dual-focus property, which is useful for the multi-focal camera modules in mobile phones and compensation devices for multi-layer optical storage [12]. Several methods to fabricate OAMLAs have been proposed, such as laser interference and photo-replication technique using birefringent materials like liquid crystalline polymer (LCP) [12,13]. Furthermore, elliptical shape of microlens array is also developed [14,15]. However, these methods require cumbersome processes to obtain unidirectionally aligned LCP or lens shapes.

A simple electrostatic technique to create lateral structures in polymer films was recently developed by using electrohydrodynamic instability (EHDI) [16–18]. Depending on the electrode structure, the EHDI method produces stripe or pillar shapes using optically isotropic organic materials on a submicrometer length scale.

In this paper, we report the fabrication of OIMLAs and OAMLAs with the same materials using EHDI and surface properties. Using patterned electrodes, we can generate EHDI and create MLAs, and the optical properties are controlled by the alignment layer, which contacts the lens materials.

2. Experiments

Figure 1 shows a schematic diagram of a fabrication process. First, we prepared a patterned electrode on an indium-tin oxide (ITO) coated glass as a master substrate to create EHDI. To produce a circular shape of MLA, the electrode is patterned as a circular shape with a diameter of 40 μm using a photolithographic technique. The circular pattern arrays are connected each other with the thin lines of 5 μm width for applying the electric field. After the cleaning process, a solution of reactive mesogen (RM) (RMS03-001C, Merck) is spin-coated on the master substrate. RM is a liquid crystalline material that can be permanently fixed in the liquid crystal phase by polymerization. The ordinary and extraordinary refractive indices of used RM are 1.525 and 1.68, respectively. The initial thickness of the RM layer measured by the surface profiler is about 1.5 μm. To evaporate the solvent, it is heated at 60 °C for 3 minutes. Subsequently, the non-patterned substrate is spin-coated with an alignment material and placed under the master substrate as a transfer substrate with a gap of 5.5 μm by using glass spacers which are commonly used at liquid crystal display (LCD) processes, as shown in Fig. 1(a). By controlling of alignment of the RM in the MLA structure, we can control the optical properties of the MLA. In order to make the OAMLA, we use two different planar alignment layers (AL22620 from JSR and RN1199 from Nissan) that are rubbed unidirectionally by a velvet cloth. OIMLA can be achieved by using homeotropic alignment layer (AL1H659 from JSR).

When we apply an electric field larger than 4×10^6 V/m at 1 kHz for 10 seconds at room temperature, a pillar array on the electrode area is formed due to the EHDI, as shown in Fig. 1(b). Such a high electric field produces an electrostatic pressure ($p_{el} = -\varepsilon_0 \varepsilon_{RM} (\varepsilon_{RM} - 1) E_{RM}^2$) with the infinitesimal waves of the RM layer, known as capillary waves, and amplifies them

[16]. ε_0 and ε_{RM} are the dielectric constant of the vacuum and the average value of the RM (i.e., $\varepsilon_{RM} = (\varepsilon_o^{RM} + \varepsilon_e^{RM})/2$), respectively, and E_{RM} is the effective electric field in the RM layer. The pressure is attributed to the difference of the electric field at the RM/air interface due to the different polarizabilities of RM and air. Consequently, the electrostatic forces produce a pressure gradient along the lateral direction inside the RM layer, and generate the instability and de-wetting of the RM layer. If the electrostatic pressure is larger than the surface tension of the RM, then it the RM will flow. Without electrode patterning, pillars are therefore formed in random positions. However, the microlens must be placed at a defined position in most optical devices. If we adopt a patterned electrode like the one in this study, then a non-uniform electric field is generated, and the flow of RM is focused on the electrode region that provides a large electrostatic force. This results in the formation of a pillar array at the position corresponding to the electrode region. When we remove the applied field, the pillar structure can be changed to a liquid bridge as shown in Fig. 1(c). If we remove the master (top) substrate, then the pillar structure is mechanically divided into the top and bottom substrates. The physical removing process of top substrate is not so difficult, but a proper lift will be needed for large size samples. The divided pillar structure becomes hemispherical in order to minimize the surface tension as shown in Fig. 1(d). The substrate with the hemisphere is exposed to UV (λ = 365 nm) for 5 minutes. RM monomers are polymerized by UV exposure, and the MLA is hardened and fixed on the substrate. We refer to this polymerized RM as a LCP. We note that we can fabricate various shapes of MLAs with different shape of electrode patterning.
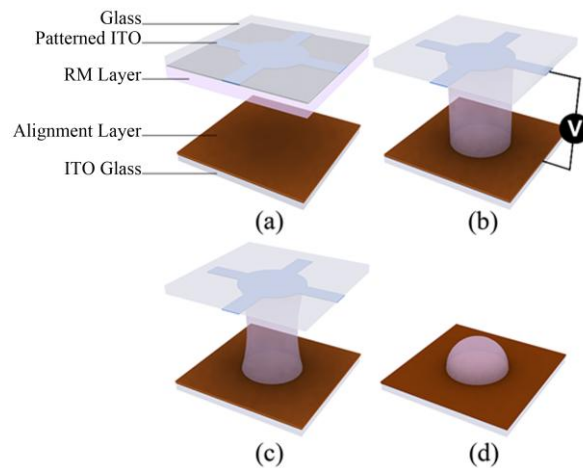

Fig. 1. Fabrication procedure of MLA fabricated by using EHDI.

3. Results and discussion

Figure 2 shows the structure obtained after removing the master substrate on two different planar alignment layers, RN1199 and AL22620. Figures 2(a) and 2(b) show the formation of a not fully separated shape of the RM layer on RN1199 and a well-defined MLA on AL22620. The contact angles of RM solutions on RN1199 and AL22620 are about 17 degrees and 27 degrees, respectively, which means that the surface tension of RM on RN1199 is higher than on AL22620. Since the MLA structure depends on the directed flow of RM, and it starts when the electrostatic forces induced by an electric field overcome the surface tension of the RM layer, RM molecules on AL22620 can flow more easily than those on RN1199 at the same electrostatic force.
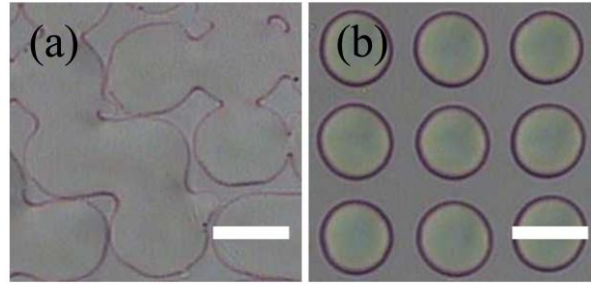
Fig. 2. The microscopic images of fabricated MLA on (a) RN1199 and (b) AL22620. The scale bars are 50 μm.

Figure 3 shows scanning electron microscope (SEM) images of pillar structures and the MLA after removal of the master substrate on AL22620, as well as a surface profile of the MLA. For SEM observations, we exposed UV after formation of the pillar structures. As mentioned above, pillar structures are formed on the electrode area due to the directed flow, as shown in Fig. 3(a). Figures 3(b) and 3(c) show a SEM image and surface profile of MLA after removal of the master substrate followed by UV exposure, respectively. The diameter and height of the microlens are about 50 μm and 3 μm, respectively. We note that we can produce MLAs with various diameters from sub-micrometers to several hundred micrometers by controlling various parameters, such as the diameters of the patterned electrode, thickness of the RM layer, distance between two substrates, and viscosity of the RM. Figure 3(d) shows the size distribution of fabricated MLA. These results confirm that our method is a highly reliable technique for the production of MLA
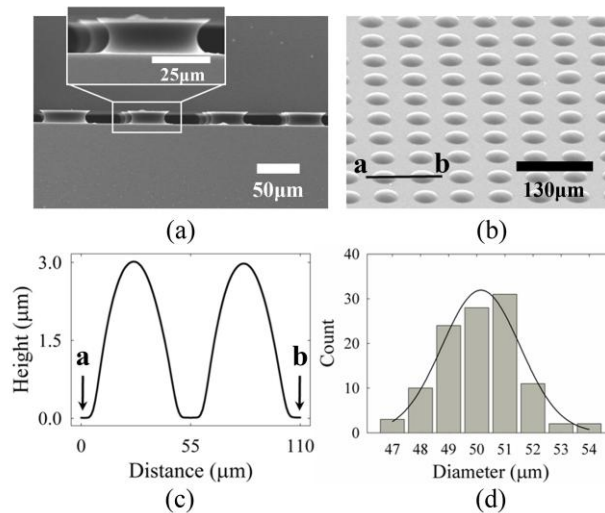

Fig. 3. SEM images of (a) cross-section and (b) top-view after forming a pillar array on the patterned electrode; (c) Surface profile from position a to b in (b), and (d) size distribution of fabricated MLA.

The other important surface property is the alignment capability of the surface. Figure 4 shows the alignment textures under crossed nicols of the MLA on planar and vertical alignment layers after UV exposure. Figures 4(a) and 4(b) show dark and bright states when the rubbing direction is 0 or 45 degrees with respect to the rubbing direction on the planar alignment layer (AL22620), respectively. This means that molecules in LCP are aligned along the rubbing direction as shown in Fig. 4(c). Since RM monomers are liquid crystalline materials before polymerization, RM molecules are homogeneously aligned in the rubbing

direction, and the UV exposure polymerizes the aligned RM monomers. Due to the birefringent property of LCP like LC, the fabricated MLA has polarization dependence; thus, we can obtain the OAMLA. On the other hand, we can observe a pinwheel texture, which does not depend on the sample rotation on the homeotropic alignment layer (AL1H659), as shown in Figs. 4(d) and 4(e). This result demonstrates that RM monomers are aligned in the vertical direction with tilting by the surface shape, as shown in Fig. 4(f). Because the LCP has symmetric alignment along the hemisphere surface, we expect OIMLA. These results demonstrate that we can easily fabricate OAMLA and OIMLA with the same material depending on the alignment capability of the surface.
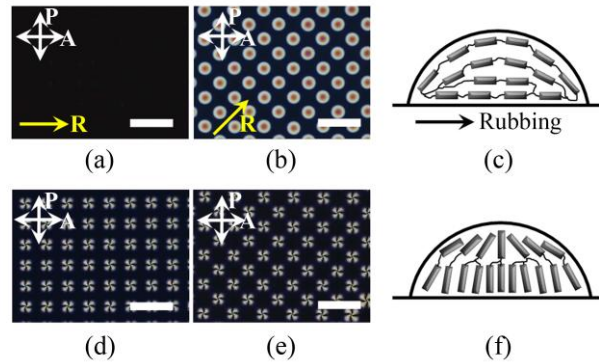

Fig. 4. The polarizing optical microscopic (POM) images for OAMLA and OIMLA: the rubbing direction is 0° in (a) and (d), and 45° in (b) and (e) with respect to the optic axis of polarizers. (c) and (d) are schematic diagrams of the alignment states of RM molecules in OAMLA and OIMLA, respectively. P, A, and R denote the polarizer, analyzer, and rubbing direction, respectively. The scale bars in POM images are 130 μm.

Figure 5 shows the focusing properties of the OAMLA and OIMLA. The focal length of the OAMLA depends on the polarization of incident light. If the optic axis of the LCP is parallel to the polarization of incident light, the light has an extraordinary refractive index of LCP ($n_e = 1.68$), and the beam is focused at 115 μm from the MLA, as shown in Fig. 5(a). When we rotate the incident polarization to 90 degrees, the focused beam is diverged and refocused at 130 μm, because the polarization of incident light is parallel to the fast axis of the LCP ($n_o = 1.525$), as shown in Figs. 5(b) and 5(c). The beam profiles measured at each focusing state are shown in Fig. 5(d). The measured profiles fit a Gaussian distribution. OIMLA does not depend on the incident polarization, because the LCP is aligned in the vertical direction as shown in Fig. 4(e). Figure 5(e) shows the intensity of the focused beam at the focal point with different polarization directions. We conclude that the MLA on the vertical alignment layer acts as an OIMLA.
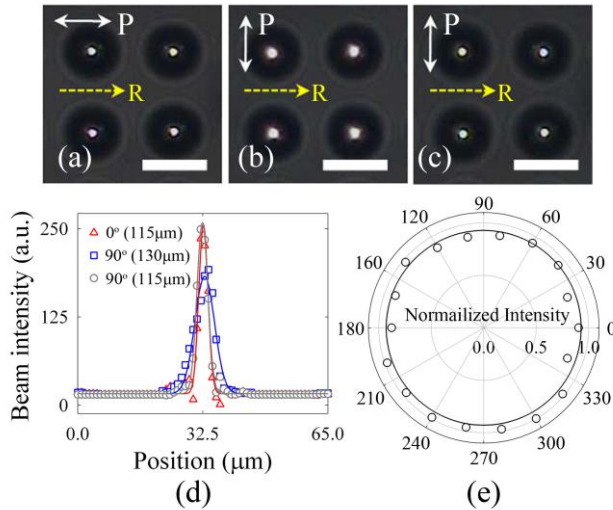
Fig. 5. Focusing properties of the OAMLA: (a) focused beam image along the optic axis of the incident polarizer at 115 μm; (b) beam image when the incident polarizer is rotated 90° with respect to the rubbing direction at 115 μm; (c) refocused beam image at 130 μm; (d) beam profiles of (a)~(c); (e) beam intensity of OIMLA at focal point as a function of the polarization state of the incident light. The scale bars in the figure are 50 μm.

4. Conclusion

In summary, we fabricated an optically isotropic and anisotropic MLA by using EHDI by taking advantage of patterned electrode and surface properties. The induced instability of the RM layer caused by a strong field leads to anisotropic flow towards the patterned electrode region. Depending on the direction of alignment, we can easily fabricate OAMLA and OIMLA. We believe that this method is a straightforward, fast, and reliable process for MLA fabrication, since it does not require cumbersome developing and molding processes.

Acknowledgment